

Non-parabolic effect for femtosecond laser-induced ultrafast electro-absorption in solids

Li-Bo Liu(刘利博)[1], Hong-Xiang Deng(邓洪祥)[1,2], Xiao-Tao Zu(祖小涛)[1], Xiao-Dong Yuan(袁晓东)[2], Wan-Guo Zheng(郑万国)[2]

Citation: Chin. Phys. B . 2020, 29(1): 017801 . **doi:** 10.1088/1674-1056/ab577c
Journal homepage: http://cpb.iphy.ac.cn; http://iopscience.iop.org/cpb

What follows is a list of articles you may be interested in

Numerical and experimental study of the mesa configuration in high-voltage 4H-SiC PiN rectifiers

Xiao-Chuan Deng(邓小川), Xi-Xi Chen(陈茜茜), Cheng-Zhan Li(李诚瞻), Hua-Jun Shen(申华军), Jin-Ping Zhang(张金平)
Chin. Phys. B . 2016, 25(8): 087201 . **doi:** 10.1088/1674-1056/25/8/087201

An improved EEHEMT model for kink effect on AlGaN/GaN HEMT

Cao Meng-Yi, Lu Yang, Wei Jia-Xing, Chen Yong-He, Li Wei-Jun, Zheng Jia-Xin, Ma Xiao-Hua, Hao Yue
Chin. Phys. B . 2014, 23(8): 087201 . **doi:** 10.1088/1674-1056/23/8/087201

Experimental and numerical analyses of high voltage 4H-SiC junction barrier Schottky rectifiers with linearly graded field limiting ring

Wang Xiang-Dong, Deng Xiao-Chuan, Wang Yong-Wei, Wang Yong, Wen Yi, Zhang Bo
Chin. Phys. B . 2014, 23(5): 057203 . **doi:** 10.1088/1674-1056/23/5/057203

Red-shift law of intense laser-induced electro-absorption in solids

Deng Hong-Xiang, Zu Hao-Yue, Wu Shao-Yi, Sun Kai, Zu Xiao-Tao
Chin. Phys. B . 2014, 23(2): 027801 . **doi:** 10.1088/1674-1056/23/2/027801

Non-parabolic effect for femtosecond laser-induced ultrafast electro-absorption in solids*

Li-Bo Liu(刘利博)[1], Hong-Xiang Deng(邓洪祥)[1,2,†], Xiao-Tao Zu(祖小涛)[1], Xiao-Dong Yuan(袁晓东)[2], and Wan-Guo Zheng(郑万国)[2]

[1] School of Physics, University of Electronic Science and Technology of China, Chengdu 610054, China
[2] Research Center of Laser Fusion, China Academy of Engineering Physics, Mianyang 621900, China

(Received 5 July 2019; revised manuscript received 5 September 2019; accepted manuscript online 14 November 2019)

A theoretical study for femtosecond laser-induced ultrafast electro-absorption of bulk solids is presented. Our numerical results show that, in the case of low intensity of the pump laser where the interaction between the pump laser and solids is in the multi-photon regime, the energy band of solids can be approximately taken as a parabolic band and electro-absorption spectrums from the parabolic band and real band are nearly the same. While, in the case of high intensity where the interaction is in the tunneling regime, spectrums from the parabolic band and real band are quite different. The physical mechanism for the difference in the tunneling regime is found. We find that the non-parabolic parts of the real energy band and Bragger scattering of electrons near the first Brillouin zone boundaries, which are neglected in previous studies, strongly influence the electro-absorption spectrum in the tunneling regime. These two physical processes cause the difference of spectrums. Our theoretical results are in accordance with the experiment result.

Keywords: ultrafast electro-absorption, red-shift of absorption edge, Bragger scattering effect, multi-photon process

PACS: 78.47.–p, 72.20.Ht, 42.65.Ky, 78.40.Fy **DOI:** 10.1088/1674-1056/ab577c

1. Introduction

Femtosecond laser has been widely used in many fields, such as laser micromachining,[1–5] laser-driven accelerators,[6] ultrafast dynamics in atoms and solids,[7,8] and laser modulation spectrum in solids.[9–12] The interaction between solids and an intense laser can cause dramatic modification of the energy band of the solids,[13] from which many interesting phenomena have been observed such as laser-induced transparency,[11] harmonic generation,[14–16] sideband generation,[9] and ultrafast electro-absorption.[12,17] Ultrafast electro-absorption of near band-gap radiation has been investigated both theoretically[18,19] and experimentally,[11,17] and the parabolic band was used to study laser ultrafast electro-absorption of bulk solids in previous works.[17] If the intensity of the pump laser is not high, the parabolic band is a good approximation for describing the energy band of real solids, since the main contribution to the band–band transition is from the electrons near the center of the Brillouin zone. However, as the pump laser becomes extremely intense, this approximation is no longer valid.[20]

Usually, the Keldysh adiabatic parameter $\gamma = \sqrt{E_g/4U_P^*}$ is employed to define the different regimes of the pump laser in laser-induced electro-absorption of bulk solids, where E_g is the band gap of the solids and $U_P^* = e^2A_0^2/4m_r$ is the ponderomotive potential, with $m_r = 1/m_c - 1/m_v$ being the reduced mass of electron and hole, and A_0 the amplitude of the vector potential of the pump laser. In the case of $\gamma \gg 1$, the intensity of the pump laser is in the multi-photon regime. In the case of $\gamma \sim 1$, the intensity is in the dynamic regime. Finally, in the case of $\gamma \ll 1$, it is in the tunneling regime. Previous experiments of ultrafast electro-absorption focused on the multi-photon regime and dynamic regime with the intensity up to the case of $U_P^* \sim \hbar\omega_0$. Here, $\hbar\omega_0$ is the photon energy of the pump laser.[12] Due to the laser-induced damage of the sample, the tunneling regime remains relatively unexplored.[12,14] Recently, Ghimire *et al.*[12] made an exploration in this regime. In their experiment, the wide band semiconductor ZnO and long wavelength laser were used to avoid damage effect on the sample. The substantial red-shift of absorption edge in ultrafast electro-absorption was observed.[12] They found that the red-shift is close to the case described by the direct current (DC) approximation from 0.1 TW/cm^2 to 1 TW/cm^2 (from dynamic regime to tunneling regime), but has an obvious deviation from 1 TW/cm^2 to 5 TW/cm^2 (deeper into the tunneling regime). The result is quite surprising. Because the traditional concept is that, in the optical tunneling regime, a pump laser can be taken as a quasi-static field and the photon effect is negligible.[17] One would expect that the more intense the laser is, the better DC approximation may apply. Ghimire *et al.* assumed that the deviation may originate from the non-parabolic band structure and Bragger scattering (BS). Considering that intense laser can easily cause sample damage, to study electro-absorption at high intensity, the sample

*Project supported by the National Natural Science Foundation of China (Grant No. 61505023).
†Corresponding author. E-mail: denghx@uestc.edu.cn
© 2020 Chinese Physical Society and IOP Publishing Ltd

should have a high damage threshold. Usually, the solids with large band gap have a high damage threshold. So, the wide band gap (also with direct gap) semiconductor and dielectric are chosen as the sample, such as GaAs, ZnO, ZnS, and quartz. In order to be consistent with Ghimire's experiment, we also choose ZnO as the sample of research.

In this work, a theoretical analysis for femtosecond laser-induced ultrafast electro-absorption of solids is presented. A general expression for electro-absorption of solids with non-parabolic band structure and BS is given and a numerical study of ZnO crystal by the expression is demonstrated. Our results show that, in the case of low intensity pump laser where the interaction between the pump laser and solids is in the multi-photon regime, the energy band of the solids can be approximately taken as a parabolic band and electro-absorption spectrums from the parabolic band and non-parabolic band are nearly the same. While, in the case of high intensity where the interaction is in the tunneling regime, spectrums from the parabolic band and real band are quite different. The physical mechanism for the difference in the tunneling regime is found. We find that the non-parabolic parts of the real energy band and Bragger scattering of electrons near the first Brillouin zone boundaries, which were neglected in previous studies, strongly influence the electro-absorption spectrum in the tunneling regime.

2. Results

2.1. General theory

Figure 1 is a setup of ultrafast electro-absorption experiment.[12] In Fig. 1, the pump laser is used to modulate the transmission or absorption spectrum of the probe laser. In the presence of the pump laser, the optical absorption process of the probe laser can happen even the photon energy of the probe laser is lower than the band gap of solids. This effect can be seen as a shift of the absorption edge to lower photon energies (red-shift of absorption edge). For ultrafast electro-absorption, the pump laser is intense and the probe laser is weak. The intensity of the pump laser is very high and will damage the detector of the probe laser if it enters the detector. In order to avoid pumping laser into the detector of the probe laser, a very small degree θ between the probe laser and pump laser (the direction of the pump laser is vertical to the sample surface) is employed in the experiment. For simplicity, it can be approximately taken as 0°.

The interaction Hamiltonian for laser-induced electro-absorption is

$$H = H_{\mathrm{e-pump}} + H_{\mathrm{e-probe}}, \tag{1}$$

where $H_{\mathrm{e-pump}}$ and $H_{\mathrm{e-probe}}$ are Hamiltonian of the electron–pump laser interaction and Hamiltonian of the electron–probe laser interaction, respectively.

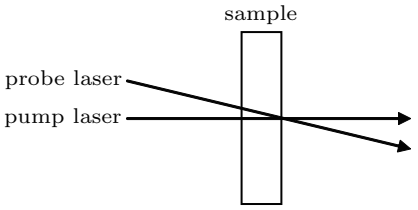


Fig. 1. Setup of laser-induced electro-absorption. The pump laser is intense and the probe laser is weak.

For an intense laser, it is necessary to treat the interaction between the laser and an electron non-perturbatively.[21–24] In ultrafast electro-absorption, the electron inside each energy band is accelerated by the pump laser and the energy of the electron on the i-th band is $E_i(\boldsymbol{p}+e\boldsymbol{A}_0\cos(\omega_0 t))$ (velocity gauge), where $\boldsymbol{p}$ is the quasi momentum of the electron; $\boldsymbol{A}_0\cos(\omega_0 t)$ the laser vector potential of the pump laser; and $E_i(\boldsymbol{p})$ the energy of the electron without laser. Substituting the energy $E_i(\boldsymbol{p}+e\boldsymbol{A}_0\cos(\omega_0 t))$ into the Schrödinger equation, we have

$$\begin{aligned}\psi_{\mathrm{C}} &= \phi_{\mathrm{C}}(\boldsymbol{r})\exp\left(\mathrm{i}\boldsymbol{p}\cdot\boldsymbol{r} - \int_0^t E_{\mathrm{C}}(\boldsymbol{P}(\tau))\,\mathrm{d}\tau\right),\\ \psi_{\mathrm{V}} &= \phi_{\mathrm{V}}(\boldsymbol{r})\exp\left(\mathrm{i}\boldsymbol{p}\cdot\boldsymbol{r} - \int_0^t E_{\mathrm{V}}(\boldsymbol{P}(\tau))\,\mathrm{d}\tau\right),\end{aligned} \tag{2}$$

where ψ_{C} and ψ_{V} are the wave functions of the conduction band and valence band, respectively; $\boldsymbol{P} = \boldsymbol{p} + e\boldsymbol{A}_0\cos(\omega_0 t)$; and $\phi_{\mathrm{C}}(\boldsymbol{r})$ and $\phi_{\mathrm{V}}(\boldsymbol{r})$ are functions that have the translational symmetry of the lattice. The energy $E_i(\boldsymbol{P})$ (one dimension as an example) can be expanded as

$$E_i(\boldsymbol{P}(t)) = E_i(0) + \left(\frac{\mathrm{d}E_i}{\mathrm{d}P}\right)_{P=0} P + \frac{1}{2}\left(\frac{\mathrm{d}^2E_i}{\mathrm{d}P^2}\right)_{P=0} P^2 + \cdots.$$

If effective mass approximations $\mathrm{d}^n E_i/\mathrm{d}P^n = 0\,(n \neq 2)$ and $\mathrm{d}^2E_i/\mathrm{d}P^2 = 1/m_i^*$ are used, we have $E_i(\boldsymbol{P}(t)) \approx E_i(0) + \frac{(\boldsymbol{p}+e\boldsymbol{A}_0\cos(\omega_0 t))^2}{2m_i^*}$, here m_i is the effective mass in the i-th band. In this approximation, equation (2) reduces to the Bloch–Volkov wave-function.[17]

Since the Hamiltonian of the electron–probe laser interaction is rather weak, it can be taken as a perturbation. The transition probability amplitude C_{f} from the valence band to the conduction band caused by the probe laser now is in the form

$$\begin{aligned}C_{\mathrm{f}} &= \frac{1}{\mathrm{i}\hbar}\int_0^t\int \psi_{\mathrm{C}}^* H_{\mathrm{el}}\psi_{\mathrm{V}}\,\mathrm{d}\boldsymbol{r}\,\mathrm{d}t'\\ &= \frac{1}{\mathrm{i}\hbar}\int_0^t \mathrm{d}t' H_{\mathrm{CV}}\exp\left\{\frac{\mathrm{i}}{\hbar}\int_0^{t'}\left(E_{\mathrm{C}}(t'') - E_{\mathrm{V}}(t'')\right) - \hbar\omega\,\mathrm{d}t''\right\},\end{aligned} \tag{3}$$

where $H_{\mathrm{el}} = \frac{\boldsymbol{A}\cos(\omega t)\cdot\boldsymbol{p}}{m_{\mathrm{e}}}$ is the Hamiltonian of the electron–probe laser interaction. Here, m_{e} is the mass of free electron; $\boldsymbol{A}\cos(\omega t)$ is the laser vector potential of the probe

laser; $H_{\mathrm{CV}} = \int \psi_{\mathrm{C}}^{*} H_{\mathrm{el}} \psi_{\mathrm{V}} |_{t=0} \mathrm{d}\boldsymbol{r}$. Similar to the treatment in Ref. [21], we now expand the following expression in Eq. (3):

$$L\left(t'\right) = H_{\mathrm{CV}} \exp\left\{\frac{\mathrm{i}}{\hbar}\int_{0}^{t'}\left(E_{\mathrm{C}}\left(t''\right) - E_{\mathrm{V}}\left(t''\right)\right) - \hbar\omega\,\mathrm{d}t''\right\} \quad (4)$$

in a Fourier series of t'

$$L\left(t'\right) = \sum_{n=-\infty}^{\infty} \exp\left\{\frac{\mathrm{i}}{\hbar}\left(E_{\mathrm{eff}} - \hbar\omega\right)t'\right\} \exp\left(-\mathrm{i}n\omega_0 t'\right) L_n, \quad (5)$$

where

$$L_n = H_{\mathrm{CV}} \frac{1}{2\pi}\int_{-\pi}^{\pi} \exp\left\{\frac{\mathrm{i}}{\hbar}\int_{0}^{t'}\left(E_{\mathrm{C}}\left(t''\right) - E_{\mathrm{V}}\left(t''\right) - E_{\mathrm{eff}}\right)\mathrm{d}t''\right\} \times \exp(\mathrm{i}nx)\,\mathrm{d}x.$$

Here, $x = \omega t'$; $E_{\mathrm{eff}} = \frac{1}{2\pi}\int_{-\pi}^{\pi} E_{\mathrm{C}}(x) - E_{\mathrm{V}}(x)\,\mathrm{d}x$ is the effective band difference between the effective conduction band $\frac{1}{2\pi}\int_{-\pi}^{\pi} E_{\mathrm{C}}(x)\,\mathrm{d}x$ and the effective valence band $\frac{1}{2\pi}\int_{-\pi}^{\pi} E_{\mathrm{V}}(x)\,\mathrm{d}x$. Substituting Eq. (5) in Eq. (3) and then using the same calculation procedure used in the normal perturbation theory,[21] we obtain the transition rate for the absorption of the probe laser in the form (the spin states of the electron are considered)

$$W = \sum_{n} \frac{2\pi}{\hbar}\int |L_n|^2 \delta\left(E_{\mathrm{eff}} - n\hbar\omega_0 - \hbar\omega\right)\frac{2}{(2\pi)^3}\,\mathrm{d}\boldsymbol{k}, \quad (6)$$

where $\hbar\omega_0$ and $\hbar\omega$ are the photon energies of the pump laser and the probe laser, respectively. In Eq. (6), the expression $\frac{2\pi}{\hbar}\int |L_n|^2 \delta\left(E_{\mathrm{eff}} - n\hbar\omega_0 - \hbar\omega\right)\frac{2}{(2\pi)^3}\,\mathrm{d}\boldsymbol{k}$ describes the transition process of absorbing n pump photons and one probe photon. The absorption coefficient of the probe laser that is caused by this band–band transition now can be written as

$$\alpha = \frac{\omega}{n_{\mathrm{r}} c\omega\varepsilon_0}\frac{2W\hbar\omega}{E_{\mathrm{pro}}^2} = \frac{2W\hbar\omega}{n_{\mathrm{r}} c\varepsilon_0 E_{\mathrm{pro}}^2}, \quad (7)$$

where ε_0 is the permittivity of vacuum; c the light speed in vacuum; n_{r} the refractivity of solids; and E_{pro} is the amplitude of the electrical field of the probe laser. In Ghimire's work, ZnO (wurtzite structure) was employed in the experiment. In the present study, we use the same material to make analysis. The energy band of ZnO is adopted from the *ab initio* calculation.[25] The orientation of the reciprocal lattice of ZnO is chosen as $x \| \Gamma - M$ (polarization direction of pump laser), $y \| \Gamma - K$, $z \| \Gamma - A$ (optical axis). The conduction and valence bands structure in the polarization direction (x direction) of the pump laser is close to cosine band $E_i(k) = \frac{\hbar^2}{m_i^* \mathrm{d}^2}\left[1 - \cos(kd)\right]$, where m_i is the band effective mass at zone center in the i-th band; and d is the lattice constant.[14] The above cosine bands are periodic functions of the reciprocal lattice vector. If the wave vector of electron in the x direction k_x is out of the first Brillouin boundary, we have $E_i(k_x) = E_i(k_x - K_{\mathrm{hx}})$, here K_{hx} is the reciprocal lattice vector in the x direction. Thus, the BS effect is naturally included in the cosine band. The parabolic band and Kane band are not periodic functions, so the BS effect is not included in these band models. Since there are no acceleration effects in x and y directions, we take the parabolic approximation into these two directions.[24] In our calculation, the wavelength of the pump laser is taken as 3250 nm, which is the same as that used in the experiment.

Equation (6) indicates that the transition rate is dependent on the effective band difference E_{eff} and the mixed multi-photon process of the pump laser and the probe laser. In general, in the case of a process with low intensity laser, the lowest order of multi-photon process makes the most contribution to the transition and the contributions of higher orders can be neglected. However, in the high intensity case, the higher orders become more and more important to the transition.[23,26,27] Figure 2 is a schema for the band–band transition of ultrafast electro-absorption at different pump laser intensities. For low laser intensity, the main contribution to the inter-band transition is made by the electrons near the center of the Brillouin zone ($\boldsymbol{k} = 0$). So the parabolic band can be used to replace the real band. Whereas, at high intensity, the higher-order multi-photon processes of the pump laser are important and all electrons in the entire Brillouin zone make effective contributions (not only the electrons near the center of the Brillouin zone). This means that the ultrafast electro-absorption in the optical tunneling regime should be a band structure related process.

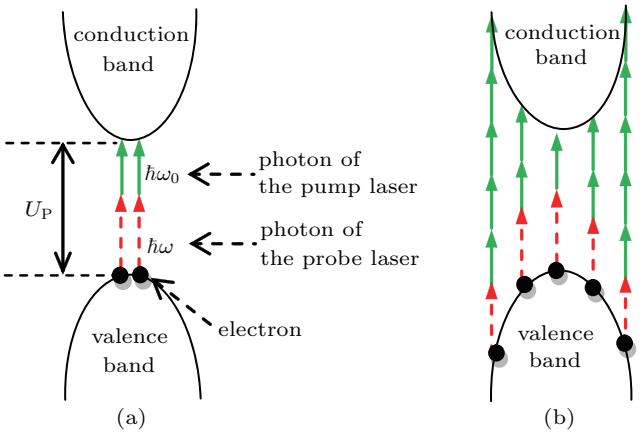


Fig. 2. Schema for the ultrafast electro-absorption: (a) the low laser intensity case and (b) the high laser intensity case.

2.2. Numerical results

In Fig. 2, U_{P} is the ponderomotive energy that also can be expressed as $E_{\mathrm{eff}}(0)$. Figure 3 shows the values of ponderomotive energy of ZnO at different pump laser intensities I, with the cosine band marked as circles and parabolic band as squares. As shown in Fig. 3, the ponderomotive energies of the cosine band and parabolic band are the same at low intensity, but quite different at high intensity. This indicates that, at high

intensity, the parabolic approximation is no longer a good approximation and the non-parabolic part of the real band needs to be considered. The ponderomotive energy has a direct connection with the phenomenon called laser-induced above band gap transparency.[11] The experiment shows that the ponderomotive energy is proportional to the intensity when the intensity of the pump laser is below the tunneling regime. It corresponds to the situation in the left of Fig. 3. It is interesting that the non-linear ponderomotive energy is found in the tunneling regime (the right part in Fig. 3). This non-linear ponderomotive energy is due to the non-parabolic band effect which is obvious, as we will show below, in the tunneling regime.

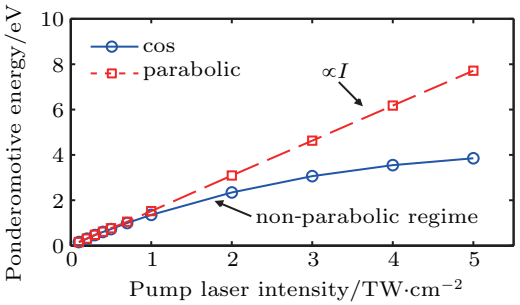


Fig. 3. Ponderomotive energy at different intensities.

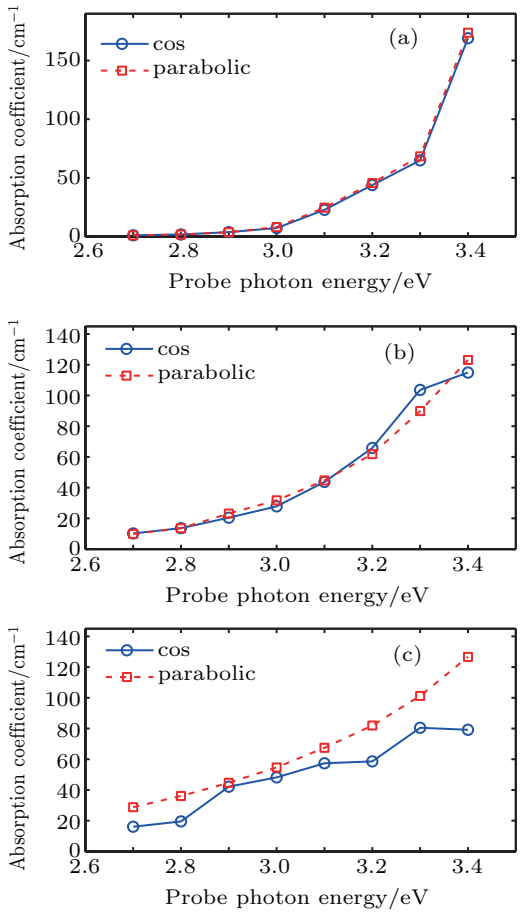


Fig. 4. Absorption coefficients of ultrafast electro-absorption at different photon energies of the probe laser. The intensity of the pump laser is (a) 0.1 TW/cm^2, (b) 1 TW/cm^2, (c) 5 TW/cm^2. Here, squares are from the parabolic band; circles are from the cosine band.

The absorption coefficients of the probe laser at different wavelengths are presented in Fig. 4. The intensities of the pump laser are 0.1 TW/cm^2, 1 TW/cm^2, and 5 TW/cm^2 in Figs. 4(a)–4(c), respectively. To make a comparison, the results from the parabolic band are also presented in Fig. 4. It directly shows that, at low intensity, the parabolic band approximation works well for describing ultrafast electro-absorption, whereas the real band structure needs to be considered at high intensity and the parabolic band is not a good approximation.

Meanwhile, we find that the curve for the cosine band presents some fluctuation in Fig. 4(c). In fact, the fluctuation has a physical origin. In Fig. 4(c), for the photon energy of the probe laser between 2.7 eV and 2.8 eV, the minimum photon number of the pump laser needed to satisfy the energy conversation in Eq. (6) is 7 (cosine band model); for the photon energy between 2.9 eV and 3.2 eV, the minimum photon number is 6; while for the photon energy between 3.3 eV and 3.4 eV, the minimum photon number of the pump laser is 5. We know that the smaller the minimum number of photons is, the easier the transition process of electron and the larger absorption coefficients. The fluctuation reflects the change of the minimum photon number of the pump laser.

The red-shift of the absorption edge of laser-induced ultrafast electro-absorption can be calculated by the same way of Franz–Keldysh effect (it corresponds to the DC case as mentioned above).[26] Supposing the point $\hbar\omega_1$ as the absorption edge of the probe laser at the pump intensity I_1, the absorption edge $\hbar\omega_2$ at the pump intensity I_2 is determined by

$$\frac{\alpha\left(\hbar\omega_1, I_1\right)}{\alpha\left(E_{\mathrm{g}}, I_1\right)} = \frac{\alpha\left(\hbar\omega_2, I_2\right)}{\alpha\left(E_{\mathrm{g}}, I_2\right)}. \tag{8}$$

It can be rewritten as

$$\frac{\alpha\left(E_{\mathrm{g}} - \Delta E_{\mathrm{g}1}, I_1\right)}{\alpha\left(E_{\mathrm{g}}, I_1\right)} = \frac{\alpha\left(E_{\mathrm{g}} - \Delta E_{\mathrm{g}2}, I_2\right)}{\alpha\left(E_{\mathrm{g}}, I_2\right)}. \tag{9}$$

Here, $\Delta E_{\mathrm{g}1} = E_{\mathrm{g}} - \hbar\omega_1$ and $\Delta E_{\mathrm{g}2} = E_{\mathrm{g}} - \hbar\omega_2$ are red-shifts of the absorption edges at the pump intensities of I_1 and I_2, respectively. For the Franz–Keldysh effect, the transition rate of the probe laser has a simple analytical expression

$$W = C\exp\left\{-\frac{4\sqrt{2m_{\mathrm{r}}}}{3e\hbar E}(E_{\mathrm{g}} - \hbar\omega)^{3/2}\right\},$$

$(\hbar\omega < E_{\mathrm{g}})$; here E is the amplitude of the external electric field.[12,26] The pre-factor C of the expression is a relatively slowly varying function of E and the frequency of the probe laser ω compared to the exponential part.[12] So we can only consider the exponential part. Using Eq. (9), we have $\Delta E_{\mathrm{g}} \propto I^{1/3}$.[27] For ultrafast electro-absorption, the expression for the transition rate of the probe laser is complicated as shown in Eq. (6). In this case, the numerical method is needed to calculate the red-shift of absorption by using Eq. (9).

Figure 5 shows the red-shift of absorption edge of ZnO at different pump intensities. In Fig. 5, solid diamonds are

from an experiment.[12] The solid squares, empty circles, and empty triangles are calculated from the cosine band, parabolic band approximation, and Kane band approximation,[21] respectively. The dash line is obtained from the DC approximation. For the DC approximation, the results from above different bands are the same. All results are listed in Table 1. For the case of DC approximation, the red-shifts of absorption edge at different energy bands have the same law $\Delta E_g \propto I^{1/3}$, here I is the intensity of the pump laser. For the case of ultrafast electro-absorption, if there is no BS effect, the red-shifts from the parabolic band and non-parabolic band (as the case of Kane band) are equal and follow the same law from the DC approximation $\Delta E_g \propto I^{1/3}$. If the BS effect is considered (as the case of cosine band), obvious deviation from the DC approximation is found when the intensity of the pump laser is above 1 TW/cm^2. This is in accordance with the experiment.[12]

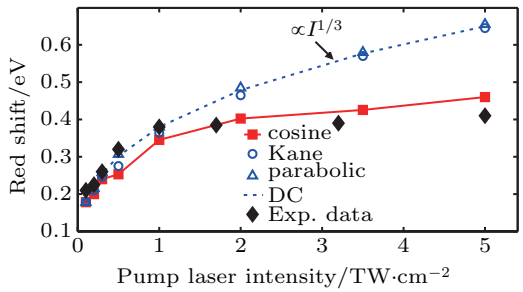


Fig. 5. Red-shift of absorption edge at different intensities. Here, solid diamonds are from the experiment; solid squares are calculated from the cosine band; empty circles and empty triangles are calculated from the parabolic band and Kane band, respectively; dash line is obtained from the DC approximation.

In Fig. 5, when the pump laser intensity is lower than 1 TW/cm^2, the cosine band model result seems not as good as those of other models. As shown in Fig. 2(a), in the case of low intensity (lower than 1 TW/cm^2), only the electrons nearby the center of the Brillouin zone make the most contribution to the ultrafast electro-absorption of direct gap solids. The parabolic and Kane band models are usually employed to describe the $E(k) \sim k$ relation nearby the center of the Brillouin zone and they are better than the description of the cosine band model in this region. This is the reason for that the parabolic and Kane band models have a better fitting effect than the cosine band model (solid squares) in the case of low intensity. Although the cosine band model has less precision to describe the $E(k) \sim k$ relation nearby the center of the Brillouin zone than the parabolic and Kane band models, it is much better to describe the $E(k) \sim k$ relation for the other parts of the energy band which are important for the case of high intensity (as shown in Fig. 2(b)) and the Bragger scattering effect of electron is naturally included in this model. So, in the case of high intensity, when the pump laser intensity is larger than 1 TW/cm^2, the cosine band model can provide a far better fitting effect compared with other models. Nevertheless, to some extent, the trend of the data of the cosine band model is still a little different from that of the experimental data. The remain difference may originate from the occupation effect of transitional electrons which is not considered in our calculation. As the laser intensity increases, the number of electrons transited from valence band to conduction band will increase. These electrons will occupy the low energy states of the conduction band, then the follow-up electrons need more energy to make the transition. This occupation effect can make a saturation trend for electro-absorption at high intensity, and the calculation result would be better if the occupation effect is considered.

3. Discussion

From Table 1, it can be found that the deviation can only happen when both the BS and the photon effect of the pump laser are considered. Figure 6 shows the influence of the BS effect in ultrafast electro-absorption. If there is no BS effect (the cases for the parabolic band and the Kane band approximations), higher order multi-photon processes in Eq. (6) are allowed to make the transition happen. However, due to the BS effect (the case for the cosine band), the high order multi-photon processes which are out of Brillouin Boundaries are forbidden. This mechanism causes the red-shift to deviate from the DC approximation. Due to this mechanism, in the tunneling regime, the pump laser cannot be simply taken as a quasi-static field.

Table 1. Summary of red-shift law of absorption edge at high intensity in Fig. 5. It can be found that only if BS and photon effect of pump laser are both considered does the deviation happen.

Energy band	Parabolic band	Kane band	Cosine band
Ultrafast electro-absorption	$\propto I^{1/3}$	$\propto I^{1/3}$	deviates $I^{1/3}$
DC approximation	$\propto I^{1/3}$	$\propto I^{1/3}$	$\propto I^{1/3}$

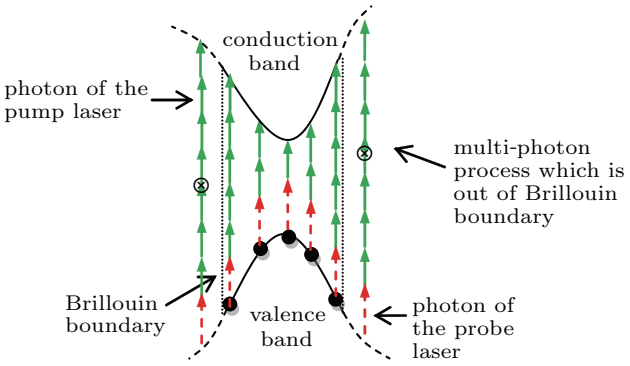


Fig. 6. Scheme for the influence of BS effect in ultrafast electro-absorption. Due to BS effect, the high order multi-photon processes which are out of Brillouin Boundaries are forbidden. This mechanism causes the red-shift to deviate from the DC approximation.

4. Conclusion

In summary, a theoretical expression for electro-absorption of solids with non-parabolic band structure and

Bragger scattering is presented and a numerical study of ZnO crystal is demonstrated. Numerical results show that, in the case of low intensity of the pump laser where the interaction between the pump laser and solids is in the multi-photon regime, the energy band of the solids can be approximately taken as a parabolic band and electro-absorption spectrums from the parabolic band and real band are nearly the same. While, in the case of high intensity where the interaction is in the tunneling regime, spectrums from the parabolic band and real band are quite different. The physical mechanism for the difference in the tunneling regime is found. We find that, in the case of tunneling regime, the non-parabolic parts of the real energy band and Bragger scattering of electrons near the first Brillouin zone boundaries which are neglected in previous studies, strongly influence the electro-absorption spectrum . These two physical processes cause the difference in the spectrums. Our results indicate that, different from the case of low intensity that the energy band of solids can be approximately taken as a parabolic band, the non-parabolic effect (non-parabolic parts of the band structure and Bragger scattering of electrons near the first Brillouin zone boundaries) should be considered for the study of electro-absorption as the interaction between the pump laser and solids is in the tunneling regime. This theoretical study can be helpful to understand the physical mechanism of intense laser-induced electro-absorption.

Acknowledgment

We really appreciate comments/suggestions given by David A. Reis (Stanford University) on the manuscript before its submission.

References

[1] Bhardwaj V R, Simova E, Rajeev P P, Hnatovsky C, Taylor R S, Rayner D M and Corkum P B 2006 *Phys. Rev. Lett.* **96** 057404
[2] Kai L, Qian S X, Wang X L, Li Y N, Gu B, Tu C H and Wang H T 2012 *Opt. Express* **20** 120
[3] Gattass R R and Mazur E 2008 *Nat. Photon.* **2** 219
[4] Li Y W, Stoica V A, Endicott L, Wang G Y, Sun H R, Pipe K P, Uher C and Clarke R 2011 *Appl. Phys. Lett.* **99** 121903
[5] Sun H Y, Luo F F, He F, Liao Y and Xu J 2010 *Chin. Phys. B* **19** 054210
[6] Hafz N A M, Jeong T M, Choi I W, Lee S K, Pae K H, Kulagin V V, Sung J H, Yu T J, Hong K H, Hosokai T, Cary J R, Ko D K and Lee J 2008 *Nat. Photon.* **2** 571
[7] Dachraoui H, Oberer C and Heinzmann U 2011 *Opt. Express* **19** 2797
[8] Fan Z F, Tan Z Y, Wan W J, Xing X, Lin X, Jin Z M, Cao J C and Ma G H 2017 *Acta Phys. Sin.* **66** 087801 (in Chinese)
[9] Chin A H, Calderón O G and Kono J 2001 *Phys. Rev. Lett.* **86** 3292
[10] Zhu Z P 2013 *Chin. Phys. B* **22** 077803
[11] Srivastava A, Srivastava R, Wang J G and Kono J 2004 *Phys. Rev. Lett.* **93** 157401
[12] Ghimire S, DiChiara A D, Sistrunk E, Szafruga U B, Agostini P, DiMauro L F and Reis D A 2011 *Phys. Rev. Lett.* **107** 167407
[13] Dunlap D H and Kenkre V M 1986 *Phys. Rev. B* **34** 3625
[14] Ghimire S, DiChiara A D, Sistrunk E, Agostini P, DiMauro L F and Reis D A 2011 *Nat. Phys.* **7** 138
[15] Faisal F H M, Kamiński J Z and Saczuk E 2005 *Phys. Rev. A* **72** 023412
[16] Vampa G, McDonald C R, Orlando G, Klug D D, Corkum P B and Brabec T 2014 *Phys. Rev. Lett.* **113** 073901
[17] Chin A H, Bakker J M and Kono J 2000 *Phys. Rev. Lett.* **85** 3293
[18] Yacoby Y 1968 *Phys. Rev.* **169** 610
[19] Jauho A P and Johnsen K 1996 *Phys. Rev. Lett.* **76** 4576
[20] Deng H X, Guo W L, Gao H H, Li L, Yuan X D, Zheng W G and Zu X T 2019 *J. Opt.* **21** 075501
[21] Keldysh L V 1964 *Sov. Phys. JETP* **20** 1307
[22] Deng H X, Zu X T, Xiang X and Sun K 2010 *Phys. Rev. Lett.* **105** 113603
[23] Deng H X, Xiang X, Zheng W G, Yuan X D, Wu S Y, Jiang X D, Gao F, Zu X T and Sun K 2010 *J. Appl. Phys.* **108** 103116
[24] Gruzdev V E 2007 *Phys. Rev. B* **75** 205106
[25] Goano M, Bertazzi F, Penna M and Bellotti E 2007 *J. Appl. Phys.* **102** 083709
[26] Keldysh L V 1958 *Sov. Phys. JETP* **7** 788
[27] Deng H X, Zu H Y, Wu S Y, Sun K and Zu X T 2014 *Chin. Phys. B* **23** 027801